STRUCTURAL ANALYSIS OF WRINKLE-RIDGE RINGS ON LUNAE AND HESPERIA PLANUM, MARS: EVIDENCE OF BURIED TOPOGRAPHY. C. R. Neel and K. Mueller, Department of Geological Sciences, University of Colorado, Boulder, CO 80309-0399

Introduction: Linear ridges (termed wrinkle ridges) located on volcanic plains of Mercury, Venus, and Mars have been interpreted as fault-related folds that accommodate crustal shortening above blind thrust faults [1, 2]. Trishear fault-propagation folding [3] has been invoked to explain wrinkle ridge morphology on Mars [4] with a steeply-sloping forelimb in the direction of fault propagation and a gently-sloping backlimb that dips similarly to the underlying fault.

The volcanic plains of Lunae Planum and Hesperia Planum (among others) contain numerous wrinkle ridges attributed to stress states caused by loading of the Tharsis complex [5, 6, 7, 8] and de-loading of Hellas Basin and loading of Tyrrhena Patera [9] , respectively. Goudy and Gregg [10] concluded that the wrinkle ridges on Hesperia Planum were formed by two different stress episodes. In addition, they indicated that the volcanic deposits covering older Noachian terrene were less than 2 km thick. Conversely, volcanic deposits that form Lunae Planum are composed of sequences of flows 3 to 5 km thick [11]. These terranes boundary conditions where wrinkle ridges have accommodated regional shortening.

Wrinkle ridges of the volcanic plains of Hesperia Planum and Lunae Planum on Mars often exhibit circular patterns (figure 1), which have been attributed to buried topography (impact craters) [12-21]. The circular ridges, termed ridge rings, are bowl-shaped and do not exhibit ejecta deposits. Previous studies have argued that wrinkle-ridge rings represent the existence of a shallow, ice-rich decollement (22). We sought to test this with an analysis of surface topography linked with kinematic models of wrinkle ridge rings. We chose Lunae Planum and Hesperia Planum as test regions because of the differences in thickness of Hesperian-aged deposits in them, which we use as a proxy for the depth to buried craters deformed by blind thrust faults.

Methodology: We developed kinematic models (figure 2) of wrinkle-ridge rings to test likely blind thrust geometeries that are affected by varying rheology including Martian megaregolith, impact-derived melt, and/or highly fractured rock that is overlain by volcanic strata. A fault wedge is generated where the hanging wall is thrust on top of the crater floor. Fault propagation occurs in two directions: 1) a backthrust that verges oppositely to the main wrinkle ridge and 2) continued thrusting in the direction of regional wrinkle ridge vergence. This model generates oppositely dipping thrust faults, which follow the curvature of the buried topography (i.e. exterior forelimbs and interior backlimbs with respect to a bowl-shaped crater).

Wrinkle-ridge rings were identified based on circularity; ring arcs and quasi-circular wrinkle ridges were not included in our analysis. The kinematic model was compared to topographic profiles of wrinkle-ridge rings at Lunae Planum and Hesperia Planum (figure 3). Topographic profiles were generated in ArcGIS software utilizing 128° per pixel MOLA-gridded topography and elevation points were collected at 500 meter increments. Profiles were examined to determine forelimb/backlimb geometry and compared to the kinematic model derived in figure 2.

Results: A typical wrinkle-ridge ring consists of 2 separate linear, parallel wrinkle ridges that arc in opposing directions to form the "sides" of the ring. A majority of the profiles (coupled with wrinkle ridge profiles along strike) indicate that backlimb/forelimb geometry switches directions from the wrinkle ridge to wrinkle-ridge ring, which we interpret to be caused by backthrusting of the blind-thrust fault at the rheologic boundary. Regional topographic offset, which is a characteristics of wrinkle ridges, is also observed through most wrinkle-ridge ring profiles.

Lunae Planum. Examination of MOLA-gridded topography identified 21 wrinkle-ridge rings; eighteen wrinkle-ridge rings displayed a morphology consistent with the kinematic model derived in figure 2. The remaining three were difficult to identify based on morphological evidence because of impact debris or intersection with another wrinkle-ridge ring.

In addition, 18 of the 21 wrinkle-ridge rings were located in the eastern half of Lunae Planum, which may indicate a thinner sequence of volcanic veneer covering Noachian-aged material in this region. A thicker sequence of volcanic flows on the western portion of Lunae may act to suppress wrinkle-ridge ring expression on the surface or subdue them such that they are not readily identifiable on MOLA data.

Hesperia Planum. Examination of MOLA-gridded topography identified 37 wrinkle-ridge rings; twenty-nine of the wrinkle-ridge rings displayed a morphology similar to the kinematic model derived in figure 2 while 2 did not fit the model. The morphology of the remaining wrinkle-ridge rings was difficult to discern for differing factors including: 1) low topographic amplitude, 2) ejecta deposits covering part of the wrinkle-ridge ring, or 3) multiple wrinkle ridges that deform or overprint the wrinkle ridge ring.

In addition to a higher number of wrinkle-ridge rings identified, Hesperia Planum also contains several high-relief scarps where faults have penetrated through Hesperian-aged volcanic deposits. These observations support a relatively thin volcanic strata in the region identified by Goudy and Gregg [10].

Discussion: Wrinkle-ridge ring morphology on Lunae Planum and Hesperia Planum suggest they form by slip on blind-thrust wedges where buried craters act as shallow strain guides. In addition, a higher density of wrinkle-ridge rings on the eastern half of Lunae Planum, and Hesperia Planum as a whole, indicates that the Hesperian-aged crust is relatively thin in these regions. Conversely, volcanic plains where wrinkle-ridge rings have not been identified (Solis Planum, for example) may have a relatively thick Hesperian-aged strata that suppresses surface expressions of these features. The intercrater volcanic plains east of Hesperia Planum also contain a higher density of wrinkle-ridge rings with respect to Lunae Planum (supporting a thin volcanic stratigraphy).

Importantly, our work suggests that wrinkle-ridge rings are not formed above shallow, weak decollements located at the depth of the buried craters. Rather, our work suggests that craters guide thrusts only at shallow levels and that these thrusts ultimately penetrate to depths comparable to those proposed for these and other regions (e.g. depths of 8.9km [23] and >10km [24]).

References: [1] Schultz R.A. (2000) *JGR, 105*, 12035-12052. [2] Golombek M.P. et al. (2001) *JGR, 106*, 23811-23821. [3] Erslev E.A. (1991) *Geology, 19*, 617-620. [4] Tate A.J. (2001) *Master's Thesis, University of Colorado,* 172p. [5] Banerdt W.B. et al. (1992) *Mars.* [6] Banerdt W.B. and Golombek M.P. (2000) *LPSC XXXI*, Abstract # 2038. [7] Phillips R.J. et al. (2001) *Science, 291*, 2587-2591. [8] Head J.W. et al. (2002) *JGR, 107,* doi:10.1029/2000JE001445. [9] Goudy C.L. and Gregg T.K.P. (2001) *LPSC XXXII*, Abstract #1393. [10] Goudy C.L. and Gregg T.K.P. (2002) *LPS XXXIII*, Abstract #1135. [11] McEwen A.S. et al (1999) *Nature, 397,* 584-586. [12] Colton G.W. et al. (1972) *NASA Spec. Pub., 315*, 4. [13] Lucchitta B. K. (1977) *8th Lunar Sci. Con.*, 2691-2703. [14] Schultz P.H. et al. (1982) *JGR, 87*, 9803-9820. [15] Chicarro A.F. et al. (1985) *Icarus, 63*, 153-174. [16] Raitala J.T. (1987) *LPS XVIII,* 812-813. [17] Schultz R.A. and Frey H.V. (1990) *JGR, 95*, 14203-14213. [18] Watters T.R. (1993) *JGR, 98*, 17049-17060. [19] Watters T.R. and Robinson M.S. (1997) *JGR, 102*, 10889-10903. [20 Kreslavsky M.A. and Basilevsky A.T. (1998) *JGR, 103*, 11103-11111. [21] Mangold N. et al. (1998) *Planet. Space Sci., 46*, 345-356. [22] Mangold N. et al. (2002) *Planet. And Space Sci., 50*, 385-401. [23] Vidal A. et al. (2005) *LPS XXXVI*, Abstract # 2333

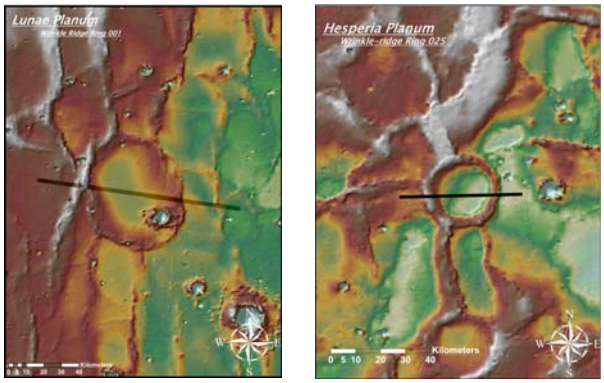

Figure 1. MOLA-gridded topography of Lunae Planum (left) and Hesperia Planum (right) indicating wrinkle-ridge rings. Selected topographic profile lines are indicated by the black transect line. The topographic scale has been stretched to obtain a distinct representation of the wrinkle-ridge ring.

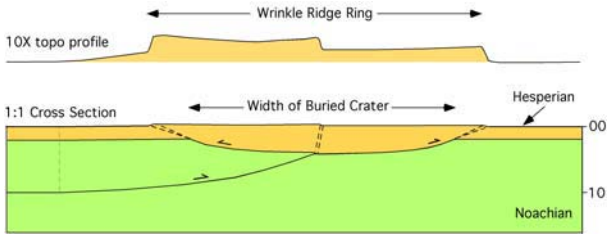

Figure 2. Schematic cross-sectional view of a blind thrust that deforms a buried crater. Note thickness of Hesperian volcanic fill relative to the 1:10 aspect ratio of buried crater and 10km thick brittle crust.

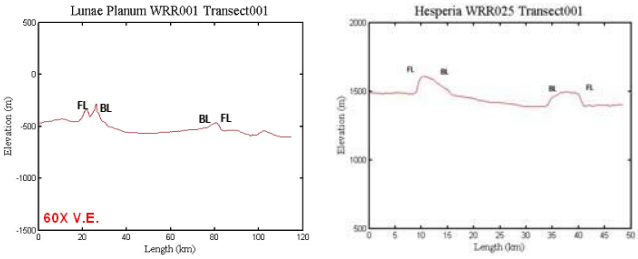

Figure 3. Topographic profiles through selected wrinkle-ridge rings in Lunae Planum (left) and Hesperia Planum (right). FL = forelimb and BL = backlimb.